Wave-function shock waves

Xiao Wang and W. E. Cooke
Department of Physics, University of Southern California, Los Angeles, California 90089-0484
(Received 26 November 1991)

When a Rydberg state is suddenly excited to an autoionizing Rydberg state by a short-pulse core-electron excitation, a shock wave is created in the Rydberg electron's wave function. This shock wave originates at small r, at the excited core, and propagates outward. This wave-function disturbance is best illustrated by the Rydberg wave function in momentum space, where the autoionization process can be seen as a filtering process that reduces the high-momentum, outgoing wave function.

PACS number(s): 32.80.Rm, 32.80.Dz

I. INTRODUCTION

Several groups have recently explored the boundary between classical and quantum-mechanical physics by considering the excitation of time-dependent, bound, Rydberg wave-packet states. These are coherent excitations of Rydberg states which evolve with a near-classical behavior. The standard preparation method uses a short pulse to excite a ground-state electron to an excited-state wave packet which begins near the origin, and then cycles out to large r and returns [1–3]. Several characteristics of these wave packets have been studied, including oscillations in their photoionization cross sections (as the packet approaches and then recedes from the small-r region) [1, 2], dephasing of the packet (since the adjacent state spacing is not constant), and nonclassical revival (since only a countable number of Rydberg states are excited) [4]. One work extended these ideas to bound Rydberg states in atoms with two electrons [5]. In that case, the Rydberg electron occasionally excites the other electron, and loses most of its energy. Eventually, the process reverses, and the system returns to a one-electron Rydberg wave packet; however, this configuration mixing modifies the normal wave-packet time evolution.

In a recent article [6], we considered what would happen when a short pulse excited the core electron of a two-electron atom in a bound Rydberg state, producing an autoionizing Rydberg wave packet. By considering only the core-electron dipole moment, we showed that it decayed in a series of "stair steps," similar to what one would expect from classical autoionization. Here, we examine the time dependence of the Rydberg-electron wave function itself, and show that it is essentially a "shock wave" which originates at the excited core, and propagates throughout the extent of the original Rydberg wave function, much like the motion of a classical particle. In this sense, this core excitation process creates a Rydberg wave-packet state, much like the bound Rydberg wave packets created in one-electron systems using photoexcitation [1–3]. However, there are major differences.

The most important experimental difference is that the core excitation process is far more efficient than photoionization, so this process will be far easier to study experimentally. In fact, the laser intensity required to saturate the core transition is two orders of magnitude lower than that used in the unsaturated one-electron photoionization experiments [6]. The most important theoretical difference is that the autoionizing shock wave decays rapidly, as autoionization depletes the Rydberg population. The perturbation introduced by exciting the core *remains* even after the exciting laser pulse has disappeared, and the continually evolving Rydberg wave is *not* periodic. Consequently, it is imperative to use a continuum of Rydberg-state wave functions, rather than the normal sum over discrete states. Here, we demonstrate a variety of ways to construct such wave functions.

Finally, we show that wave packet states better illustrate their classical behavior in *momentum space*. A bound wave function is composed of both signs of momentum at each position in space, however the time evolution of those components is very different, since they move in opposite directions. In momentum space, however, this degeneracy is unfolded, and the time evolution is monotonic, showing that the wave packet retains its essential structure, even when the spatial wave function may obscure it.

In Sec. II, we describe three methods to construct the continuum of bound Rydberg wave functions. These include explicit connection formulas for Wentzel-Kramers-Brillouin (WKB) wave functions at arbitrary energies, and a method of generating wave functions by a coordinate translation. In this section, we also illustrate that resonant core excitations generate a shock wave which follows a near-classical trajectory by evaluating the probability density flux and its local time derivative. In Sec. III, we show that the coordinate translation method of generating wave functions allows any sum over energy-dependent Rydberg wave functions to be written as a convolution, so that there is no need to construct a wave function at more than one energy. This leads to a view of the autoionization process: autoionization simply filters the wave function in the momentum space. We summarize our conclusions in Sec. IV.

II. WAVE-FUNCTION CONSTRUCTION

The basic idea of core excitation of a Rydberg state has been used for more than a decade to study the spec-

troscopy of autoionizing states [7]. An isolated core excitation (ICE) in barium, for example, might start from a $6sn'l$ bound Rydberg state, which has been excited using standard techniques, and long-pulse (5-ns) lasers. Next, a 455-nm laser would excite the $6s$ core electron to a $6p_{3/2}$ state:

$$6sn'l + \hbar\omega \rightarrow 6p_{3/2}nl. \tag{1}$$

These transitions are very efficient, since the $6s \rightarrow 6p$ transition has approximately unit oscillator strength. Consequently, it is natural to extend the ICE method by using a short pulse for the core excitation step. The only important change from the normal long-pulse ICE is that the autoionizing state will not autoionize into ions and electrons until well after the excitation pulse has disappeared.

The transition moment for this excitation of the core electron has been shown to be well described [7,8] by the product of two factors:

$$T(W) \propto \frac{\sqrt{\sinh(2\pi\gamma)/2}}{\sin[\pi(\nu+\delta+i\gamma/2)]} \frac{\sin[\pi(\nu-\nu')]}{\pi(W_\nu - W_{\nu'})}, \tag{2}$$

where ν represents the effective quantum number of the final $6p_{3/2}nl$ autoionizing state, δ is the quantum defect of the $6p_{3/2}nl$ series, γ is the scaled autoionization linewidth of the $6p_{3/2}nl$ series, and ν' represents the effective quantum number of the initial bound state. The binding energy of a state, W, is related to the effective quantum number of the state by

$$W_\nu = -\frac{1}{2\nu^2}. \tag{3}$$

Since autoionizing states decay so quickly, the uncertainty principle spreads the wave function over a large energy band, and the effective quantum number ν becomes a continuous variable (and thus the preference over the more conventional notation, n^*). This continuous ν also represents the phase of the radial wave function in multichannel-quantum-defect theory (MQDT) analyses [8]. The wave function is largest where $\nu+\delta$ is an integer, and the first factor in the transition moment of Eq. (2) is thus a resonant denominator which represents the amount of autoionizing state character in an energy region. Each peak has a full width at half maximum of γ (for small γ) when plotted *versus* ν. Since the energy spacing between Rydberg states is $1/\nu^3$, a specific ν state will have an autoionization rate of γ/ν^3. This ν dependence can be eliminated by multiplying the rate times the classical Rydberg orbit period ($2\pi\nu^3$), to identify $2\pi\gamma$ as the probability of autoionization per Rydberg orbit. This is the same for *all* n values, since autoionization only occurs when the Rydberg electron passes near the core electron, and this happens only once per orbit, regardless of the n state.

This transition moment assumes a two-channel MQDT approximation, so that the Rydberg series is not perturbed, other than through its coupling to a single continuum. Thus each Rydberg state has the same resonant value for ν, and the same probability of autoionization *per Rydberg orbit.* The wave function at each energy will then have two parts: (1) a product wave function with an excited core and a bound Rydberg electron, and (2) a deexcited core with a continuum electron. Here, we will *only* be concerned with the excited-core bound-Rydberg configuration, so that the continuum electron will never appear in our time-dependent wave functions. Moreover, we will factor out the core wave function and the angular portion of the Rydberg wave function, to construct wave functions which involve only the Rydberg radial dependence. These radial wave functions can be written as

$$\Psi_\nu(r) = \frac{\sqrt{\sinh(2\pi\gamma)/2}}{\sin[\pi(\nu+\delta-i\gamma/2)]} R_{\nu l}(r). \tag{4}$$

Here the first factor shows that the bound character increases resonantly when $\nu+\delta$ is an integer. This factor arises from the two-channel MQDT expression which distributes the bound character over a band of energies by coupling it to the continuum channel. The second factor is the bound Coulomb radial wave function. This function can be defined at *any* energy, although it will not satisfy the hydrogenic boundary conditions unless ν is an integer. Since the two-electron atom has the additional interactions between the two electrons, the boundary condition at small r can require *any* phase, depending on how strongly two configurations interact in that region. The radial wave functions in this MQDT expression are normalized per unit energy, so that

$$\int |R_{\nu l}|^2 r^2 dr = \nu^3. \tag{5}$$

The second factor of Eq. (2) arises from the projection of the initial Rydberg wave function onto the final Rydberg wave function. The two wave functions see different core potentials, so they will generally have two different phase shifts arising from their core interactions. When the core is excited, the Rydberg electron must readjust, and consequently it can change its principal quantum number.

We can now construct the time-dependent Rydberg radial wave function from the transition moment and the energy-dependent radial wave function,

$$\Psi(r,t) = \int \frac{\sinh(2\pi\gamma)}{|\sin[\pi(\nu+\delta+i\gamma/2)]|^2} \frac{\sin[\pi(\nu-\nu')]}{2\pi(W_\nu - W_{\nu'})} \times R_{\nu l}(r) e^{-iW_\nu t/\hbar} dW. \tag{6}$$

Here the integration is over energy (W), which implicitly includes an integration over ν.

In order to construct the wave-front packet, we need a continuum of bound Rydberg states. The active $6p$ core electron causes autoionization in a relatively short time, so the boundary conditions at small-r values are relaxed. There is still a preferred phase for the νl radial wave function at small r with a $6p$ ion core; however, since this configuration is mixed with continuum wave functions having a different core state, *any* phase can be accommodated. The magnitude of $6pnl$ character merely decreases as the phase deviates from the preferred value.

We have used three methods to calculate this con-

tinuum of bound radial wave functions: (1) direct integration of a time-independent Schrödinger equation, (2) WKB wave functions, and (3) a method to generate energy-shifted radial wave functions by translating the radial coordinate. The first two methods are standard; the last method provides valuable insights into the time development of the wave packet. All three methods suffer from the same difficulty—it is impossible to calculate the small-r wave function properly without introducing an energy-dependent core potential. Consequently, we have merely ignored the small-r behavior. This is in the spirit of the quantum-defect approach which leads to the transition moment and does not introduce significant errors in the wave-function probability distribution, since that is highly localized at large-r values. This approximation would be poor, however, for calculating quantities which depend on the small-r behavior (such as time-dependent photoionization of the Rydberg electron).

For all of our calculations, we have first transformed the radial coordinate to $u = \sqrt{r/2}$, so that a new radial wave function $\chi_{\nu l}$ can be defined as

$$\chi_{\nu l}(u) = 4(r/2)^{3/4} R_{\nu l}(r). \tag{7}$$

This new function then satisfies the following time-independent Schrödinger equation:

$$\left(\frac{d^2}{du^2} + 16[1 - (u/\nu)^2] - \frac{(l+\frac{1}{4})(l+\frac{3}{4})}{u^2} - 32u^2 V_c\right)\chi_{\nu l} = 0, \tag{8}$$

where ν is the effective quantum number of the state, and V_c is a short-range core potential to represent the difference between hydrogen and the multielectron system. Note that the classical turning point (at large r) occurs when $u = \nu$. For u not too large ($u \ll \nu$) and not too small ($u \gg l + 1$), this equation has the simple solution

$$\chi_{\nu l}(u) \simeq \cos(4u + \phi), \tag{9}$$

where ϕ represents a phase which must be set to match the wave function's boundary conditions so that the ratio of irregular to regular Coulomb wave functions is proportional to $\tan\phi$. A one-electron-like series of Rydberg states must have the same functional form at small u, so we can deduce that the phase ϕ depends on the energy as

$$\frac{d\phi}{d\nu} = \pi. \tag{10}$$

In our calculations, we have omitted both small-u terms (the centripetal term and the core-potential term) so that we integrated an abbreviated equation

$$\left(\frac{d^2}{du^2} + 16[1 - (u/\nu)^2]\right)\chi_\nu = 0. \tag{11}$$

This equation has the benefit that it does not diverge at small u, so that the boundary condition at small u can be ignored.

We have integrated this equation for a wide range of values of ν between 5 and 60, using a Numerov integration method with approximately 20 points per oscillation. We have normalized these wave functions per unit energy, so that

$$\int |\chi_\nu|^2 u^2 du = \nu^3. \tag{12}$$

Figure 1(a) shows an integrated wave function with a noninteger value of $\nu = 25.5$. This wave function does approach zero near the origin, because we have neglected the small-u terms in the Schrödinger equation.

Alternatively, we have used WKB wave functions to avoid the direct integration step. In the allowed region between the origin and the classical turning point ($0 < u < \nu$), Eq. (11) leads to an oscillating WKB wave function:

$$\chi_\nu \simeq \frac{\cos(2\nu\xi_1 - \nu\sin 2\xi_1 - \pi/4)}{\sqrt{\sin\xi_1}}, \tag{13}$$

where $\cos\xi_1 = u/\nu$. In the forbidden region, the decaying WKB wave function can be written as

$$\chi_\nu \simeq \frac{e^{(2\nu\xi_2 - \nu\sinh 2\xi_2 - \pi/4)}}{\sqrt{\sinh\xi_2}}, \tag{14}$$

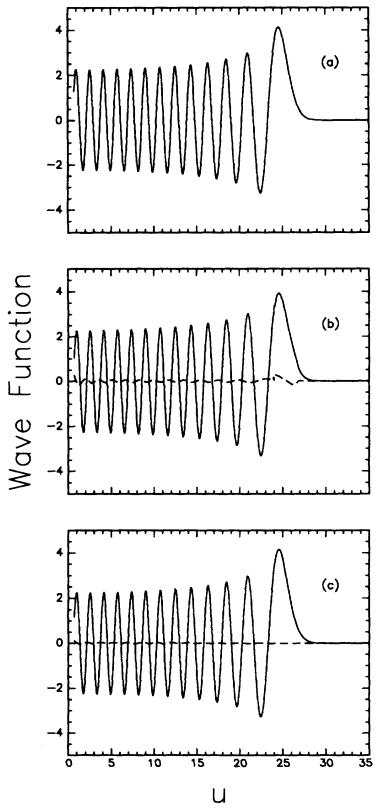

FIG. 1. The wave function $\chi(u)$ with $\nu = 25.5$, calculated three different ways: a numerical integration of Eq. (11) in (a), a WKB approximation in (b), and a coordinated shifted approximation in (c). In (b) and (c), a dashed line shows the difference between these curves and the direct integration.

where $\cosh\xi_2 = u/\nu$. These two wave functions can be matched together in a small matching region near the classical turning point, $|u-\nu| < \frac{1}{2}\nu^{1/3}$. In this connecting region, the wave function can be expanded in a power series about the turning point, in terms of yet another new variable $y = u/\nu - 1$. If one retains only the linear term in the potential expansion, then the two independent solutions each contain only every third order of y, so that

$$\chi_\nu = \frac{1}{c_1}\left[1+\alpha y^3\left(1+\frac{\alpha y^3}{5}\right)\right] - \nu c_1 y\left[1+\frac{\alpha y^3}{2}\left(1+\frac{\alpha y^3}{7}\right)\right]. \quad (15)$$

Here $\alpha = 16\nu^2/3$ and $c_1 = \frac{4}{5} + 25/\nu^2$. The two terms are independent solutions near the turning point. The relative composition of the two terms closely matches our integrated functions over the range $10 < \nu < 50$, while retaining a simple form. Figure 1(b) shows excellent agreement between the integrated wave function and the WKB composition. Typically these WKB wave functions have a normalization which is 5% too high. In Fig. (1)b, we have renormalized the WKB wave function to the correct value.

The WKB wave functions are not restricted to integer values of ν, so that all of these equations remain valid for intermediate and large u for all values of the effective quantum number (including noninteger values). Nevertheless, they are not ideal for calculating wave packets. In order to integrate the transition moment over all energy ranges using WKB wave functions, it is necessary to divide the integral into three different ranges, with the boundary between ranges changing with energy.

The final method is the least accurate, but perhaps the most instructive, and certainly the easiest calculationally. Here, we have used one correct wave function (obtained using either of the two previous methods), and then constructed new wave functions at different energies by using a coordinate translation. Near the turning point, the functional form of the wave function changes slowly as energy shifts through a change $\Delta\nu$, except that the classical turning point moves. At small u, where the wave function is approximately a cosine function, such an energy shift only introduces a phase shift, equivalent to shifting the coordinate u by $\Delta u = (\pi/4)\Delta\nu$. Thus, one expects that the change in the wave function with energy can be written as

$$u' = u + \Delta\nu f(u), \qquad \chi_{\nu'}(u) = \chi_\nu(u'), \quad (16)$$

where $f(u)$ is a function which varies slowly from $\pi/4$ at $u = 0$ to 1 at $u = \nu$. One can obtain an approximation for f by forcing the phase of the oscillating WKB wave function to be constant for changes where $du = f(u)d\nu$,

$$f(u) \simeq \frac{1}{2}\left(\frac{\xi}{\sin\xi} + \cos\xi\right), \quad (17)$$

where again $\cos\xi = u/\nu$. This can be improved and extended to values of $u > \nu$, by deriving an equation for $f(u)$ from an expansion about the turning point. Note that

$$\chi_\nu''(u') = [1+\Delta\nu f'(u)]^2\chi_\nu''(u') + \Delta\nu f''\chi_\nu'(u'). \quad (18)$$

One can choose $f(u)$ so that $\chi_{\nu'}$ satisfies an equivalent equation, given that χ_ν already satisfies Eq. (11). If we force $f(u)$ to satisfy the boundary conditions, $f(0) = \pi/4$ and $f(\nu) = 1$, and require that $f''(\nu) = 0$ to minimize errors at the turning point, then we obtain the following simple polynomial expansion for $f(u)$:

$$f(u) \simeq \left[1+\left(\frac{\pi}{4}-1\right)(1-u/\nu) + \left(\frac{2}{3}-\frac{\pi}{4}\right)(u/\nu)(1-u/\nu)(2-u/\nu)\right], \quad (19)$$

where the coefficients are *independent* of ν. This representation produces even better results than the trigonometric version derived from the WKB wave function, because this polynomial corrects for the slight phase shifting created by the variation of the amplitude of the wave function.

In Fig. 1(c), we also show a comparison between an in-

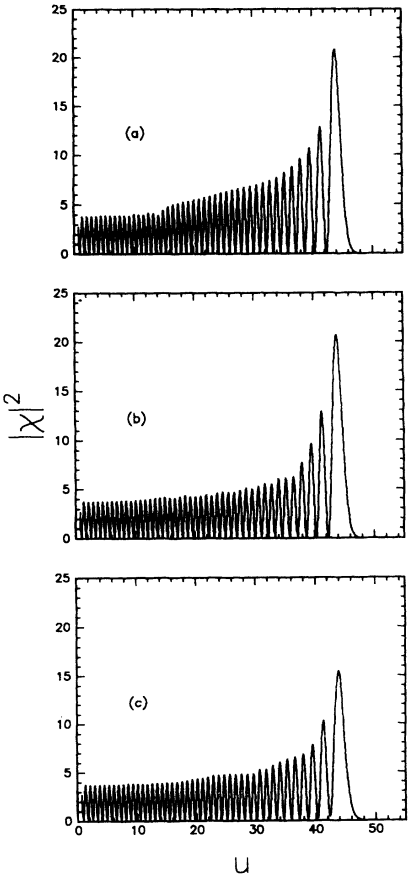

FIG. 2. The probability density ($|\chi|^2$) of the Rydberg electron at $t = 0.05$ (a), $t = 0.2$ (b), and $t = 0.5$ (c) after the core has been excited. The times are measured in fractions of the classical Rydberg orbit period.

tegrated wave function and one calculated by shifting the coordinate of a $\nu = 26$ wave function to make a $\nu = 25.5$ wave function. If we generate a $\nu = 59$ wave function by shifting the coordinate of a $\nu = 60$ wave function, the difference between the true wave function and the coordinate-shifted wave function has less than 10^{-6} probability. For large differences, such as shifting a $\nu = 60$ wave function to generate a $\nu = 30$ wave function, the remaining probability rises to a few percent. Presumably this error arises from a mismatch of the amplitudes, since we have included *nothing* to adjust the amplitude directly. Instead we have only adjusted the phase, and found that the amplitude naturally follows over a considerable range of ν.

With these wave functions, we can then generate the time-dependent wave packet according to Eq. (6). Figure 2 shows the result of our calculation for times $t = 0.05$, 0.2, and 0.5 Rydberg cycles after the initial core excitation, where we have plotted the square of the complex wave function. The wave function starts as a duplicate of the bound Rydberg state, and then a disturbance grows at the origin and travels out similar to the classical motion of a Kepler orbit. In Fig. 3, we have plotted a perspective view of the true *complex* wave function just before, and 0.01 Rydberg periods after the core excitation. From this, the disturbance appears as an eccentric spiral. At large-u values the wave function remains undisturbed yet, as the original planar wave function.

To reduce this complexity to a more instructive two-dimensional representation, we have calculated the quantum current, or flux, of these wave functions:

$$\Phi = \frac{i}{2}\left(\chi\frac{\partial\chi^*}{\partial u} - \chi^*\frac{\partial\chi}{\partial u}\right). \tag{20}$$

This current is pure real, and it is zero unless the wave function is composed of more ingoing waves than outgoing waves (or *vice versa*). In Fig. 3, the current essentially represents the cross-sectional area of the spiraling wave function. Figure 4 shows this current as a function of u at the same three times after the initial excitation as shown in Fig. 2, $t = 0.05$, 0.2, and 0.5. The dominant feature of these curves is the sharp boundary where the flux suddenly decreases. This can be identified by taking the derivative of the current, which is simply related to the local time derivative of the square of the wave function:

$$\frac{\partial\Phi}{\partial u} = \frac{i}{2}\left(\chi\frac{\partial^2}{\partial u^2}\chi^* - \chi^*\frac{\partial^2}{\partial u^2}\chi\right) = -\frac{\partial}{\partial t}|\chi|^2. \tag{21}$$

Figure 5 shows the gradient of the flux in a three-

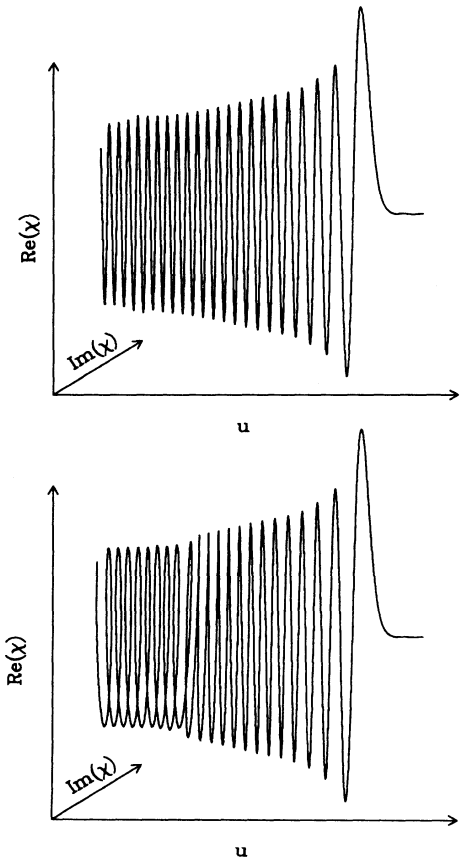

FIG. 3. Graphs of the complex $\nu = 25$ Rydberg wave function before (a), and 0.01 Rydberg periods after (b) excitation of the core. The axis going into the page shows the imaginary part of the wave function. The spiraling at low u shows that the ingoing and outgoing momenta have become unbalanced.

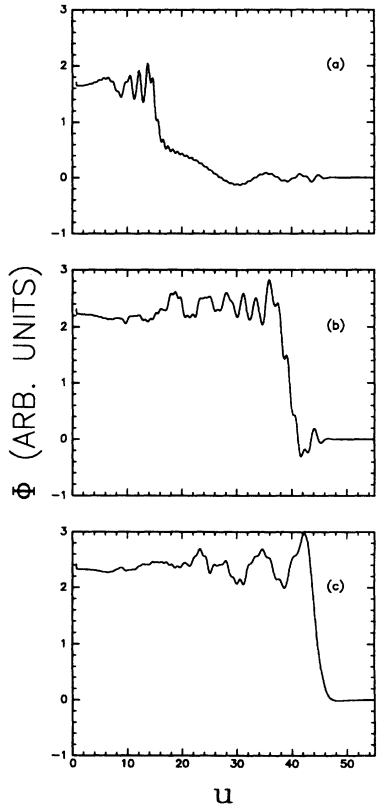

FIG. 4. The flux of the complex wave function at $t = 0.05$, 0.2, and 0.5 Rydberg cycles after the core excitation.

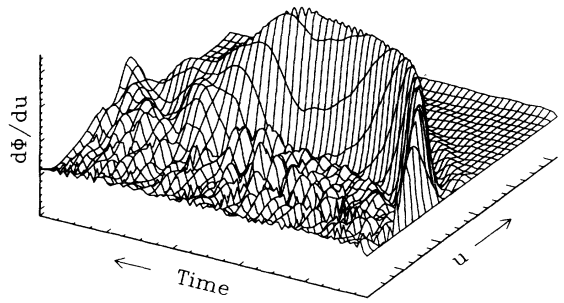

FIG. 5. The gradient of the flux as a function of time and u during the first cycle after the core excitation.

dimensional, perspective graph as a function of both u and time. This shows that the wave function changes as a local depression, or shock wave, starts at small u, and travels out, roughly following a classical trajectory. For later times, this behavior continues with a reduced amplitude, since much of the wave function has autoionized. The detail becomes less clear at smaller-u values, where the dispersion due to nonequal spacing of the low-lying levels destroys the coherence necessary for a clean pulse.

III. DISCUSSION

After a sudden core excitation, the time evolution of a Rydberg wave function gives a clear demonstration of the

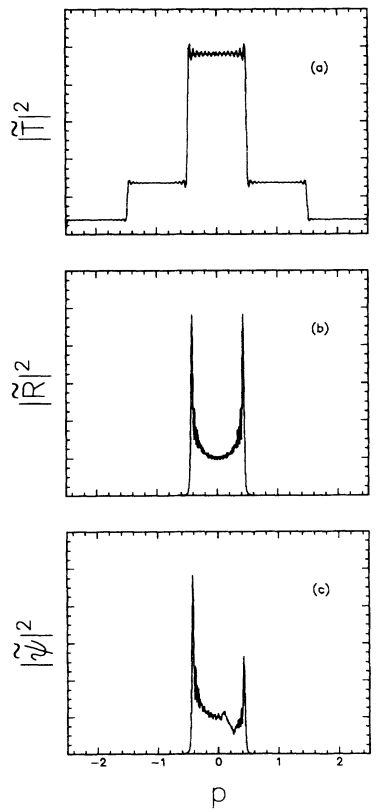

FIG. 6. The magnitudes of Fourier transforms: (a) $|\tilde{T}|^2$, (b) $|\tilde{R}|^2$, and (c) $|\tilde{\psi}|^2$ evaluated after 0.25 Rydberg cycles.

time dependence of autoionization. Initially, the excited wave function is identical to the unexcited wave function, but as time develops part of the wave function autoionizes. Physically, the part of the wave function which ionizes *must* be that part which *approaches* the small r, core region, where the excited core wave function lies. Thus, autoionization occurs at small r, but only to that part of the wave function which *enters* the core region, not to that small-r portion which is *leaving* the core. This suggests that the best way to study time-dependent autoionization is by examining the Fourier transform of the wave function—which separates the incoming and outgoing parts naturally—by the sign of the momentum.

But the Fourier transform of Eq. (6) can be simplified greatly by considering the implications of the coordinate-shifting method of constructing wave functions. If one uses the coordinate-shifting method to construct basis functions, then the sum over different energy wave functions becomes a *convolution* integral. The scaling function $f(u)$ must be eliminated by further scaling u to be $w = u/f(u)$; however, this only slightly changes the scaling of the frequency components in the Fourier transform, and does not change its essential form. With this, the Fourier transform of the total wave function can be written as the product of a Fourier transform of a single Rydberg wave function times the Fourier transform of the time-dependent coefficients, as follows:

$$\begin{aligned}
\Psi(w,t) &= \int T(\nu)\chi(w-\nu)e^{-i2\pi\nu t}d\nu, \\
\tilde{\Psi}(p) &= \int e^{-i2\pi pw}\Psi(w,t)dw = \tilde{R}(p)\tilde{T}(p+t), \\
\tilde{T}(p) &= \int e^{-i2\pi p\nu}\frac{\sinh(2\pi\gamma)}{|\sin[\pi(\nu+\delta+i\gamma/2)]|^2} \\
&\quad \times \frac{\sin[\pi(\nu-\nu')]}{2\pi(\nu-\nu')}d\nu, \\
\tilde{R}(p) &= \int e^{-i2\pi pw}\chi_\nu(w)dw.
\end{aligned} \tag{22}$$

We have used the variable p, because the Fourier transform of a coordinate space wave function is a momentum space wave function (although here we have used a scaled spatial coordinate, w). Note, however, that the variable p in the definition of $\tilde{T}$ is equivalent to time measured in units of the Rydberg cycle. Thus, time advances in Eq. (6), by shifting p in $\tilde{T}(p)$. Figure 6 illustrates this graphically. Figure 6(a) shows the Fourier transform of the transition moment, $\tilde{T}$, which is composed of a decreasing series of "stair steps," constant over one Rydberg orbit period, but decreasing after each period to show autoionization. Figure 6(b) shows the Fourier transform of the Rydberg wave function. For higher-n states, the small-p region increases and has more oscillations. The turning points in Fig. 6(b) represent the largest values of p, which are n independent and occur at the smallest-r values. Using the approximate solution of Eq. (9), and the small-u value of the scaling function, the turning points occur at $p = \pm\frac{1}{2}$.

Thus, at small times, the product $\tilde{T}\tilde{R}$ has the same

form as $\tilde{R}$, and so the wave function is unchanged. However, as t increases, $\tilde{T}(p+t)$ shifts to the left, and *decreases* the high, outgoing momentum values. This is because only outgoing waves have already autoionized; ingoing waves do not yet know that the core is excited. As time progresses, more and more momentum components are reduced, as $\tilde{T}(p+t)$ shifts farther. Physically, this is because the reduced-amplitude, high-momenta outgoing waves are slowing down in the potential, producing reduced amplitude in the lower-momenta outgoing waves. Eventually the outgoing waves arrive at their turning point, reverse, and the reduction of the wave function spreads to the ingoing waves. This is shown schematically in Fig. 6(c), where the Fourier transform of a wave function at $t = 0.25$ Rydberg periods clearly shows the reduced momenta components.

Eventually, the shock wave front returns to the core region and has yet another chance to autoionize. However, since the autoionization reduces all incoming waves by a constant fraction of their amplitude, the shock wave will persist — albeit at a reduced amplitude. Thus the wave function maintains an imbalance in momenta. It always has a net flux inward.

This itself can produce unusual atomic characteristics. For example, since the incoming and outgoing momenta components are unbalanced, the radiative couplings of this packet may be substantially different from those of a normal state. A Cooper minimum [9] occurs when the radiative transition moment passes through a zero as it changes sign. Such a zero can be thought of as a cancellation of the transition moment due to ingoing waves with that of outgoing waves. If the outgoing waves are reduced, then the fluorescence rate could increase as the cancellation is disturbed. This would be an example of an atomic system which emits, but does not absorb, radiation, in apparent violation of the normal relationship between Einstein A and B coefficients [10]. However, since this system is necessarily transient, such violations are allowed. This is similar to "lasing without inversion" schemes [11] where a cancellation between bound-bound and bound-continuum transitions is disturbed when no continuum is present; however, this case requires no coupling to the continuum at all since the cancellation occurs between the two opposite sign momentum parts of the bound wave function itself.

IV. CONCLUSION

By using a sudden core excitation to initiate autoionization in a Rydberg state, autoionization can be studied as a time-dependent process. Here we have shown that autoionization proceeds as a momentum filter, reducing outgoing high-momentum components, which then evolve throughout the entire wave function. This process creates a *shock wave* in the Rydberg wave function, which propagates as a classical particle. This shock wave presents numerous possibilities for further exploration. For example, when the shock wave returns to the core region, it will scatter from the core showing all the effects of configuration interactions — *as time-dependent interactions.*

Perhaps the most interesting use for shock waves will occur if they are transferred *back* to the bound spectra by using a second short pulse core *deexcitation.* This should produce interesting, dynamic structure in the bound atom.

ACKNOWLEDGMENT

This work was supported by the National Science Foundation under Grant No. PHY88-14903.

[1] J. Parker and C.R. Stroud, Jr., Phys. Rev. Lett. **56**, 716 (1986).

[2] A. ten Wolde, L.D. Noordam, H.G. Muller, A. Lagendijk, and H.B. van Linden van den Heuvell, Phys. Rev. Lett. **61**, 2099 (1988).

[3] G. Alber, H. Ritsch, and P. Zoller, Phys. Rev. A **34**, 1058 (1986).

[4] J.A. Yeazell, M. Mallalieu, and C.R. Stroud, Jr., Phys. Rev. Lett. **64**, 2007 (1990).

[5] W.A. Henle, H. Ritsch, and P. Zoller, Phys. Rev. A **36**, 683 (1987).

[6] Xiao Wang and W.E. Cooke, Phys. Rev. Lett. **67**, 976 (1991).

[7] W.E. Cooke, T.F. Gallagher, S.A. Edelstein, and R.M. Hill, Phys. Rev. Lett. **41**, 178 (1978); S.A. Bhatti, C.L. Cromer, and W.E. Cooke, Phys. Rev. A **24**, 161 (1981); N.H. Tran, P. Pillet, R. Kachru, and T.F. Gallagher, *ibid.* **29**, 2640 (1984).

[8] W.E. Cooke and C.L. Cromer, Phys. Rev. A **32**, 2735 (1985).

[9] U. Fano and J.W. Cooper, Rev. Mod. Phys. **40**, 441 (1968).

[10] Rodney Loudon, in *The Quantum Theory of Light* (Oxford University Press, Oxford, 1983), p. 16.

[11] S.E. Harris, Phys. Rev. Lett. **62**, 1033 (1989).